Deformed shell effects in ^{48}Ca+^{249}Bk quasifission fragments

K. Godbey and A.S. Umar*
Department of Physics and Astronomy, Vanderbilt University, Nashville, Tennessee 37235, USA

C. Simenel†
Department of Theoretical Physics and Department of Nuclear Physics, Research School of Physics and Engineering, The Australian National University, Canberra ACT 2601, Australia

(Dated: June 12, 2019)

Background:

Purpose:

Methods:

Results:

Conclusions:

PACS numbers: 21.60.-n,21.60.Jz

I. INTRODUCTION

Quasifission occurs when the collision of two heavy nuclei produces two fragments with similar characteristics to fusion-fission fragments, but without the intermediate formation of a fully equilibrated compound nucleus [1–3]. It is the main mechanism that hinders fusion of heavy nuclei and then the formation of superheavy elements [4–7]. It is then crucial to achieve a deep understanding of quasifission in order to minimize its impact and maximize the formation of compound nuclei for heavy and superheavy nuclei studies.

Quasifission also provides a unique probe to quantum many-body dynamics of out-of-equilibrium nuclear systems. For instance, quasifission studies bring information on mass equilibration time-scales [8–10], on shell effects in the exit channels [11–15], as well as on the nuclear equation of state [16, 17].

In fusion-fission, the exit channel is essentially determined by the properties of the compound nucleus, and does not depend a priori on the specificities of the entrance channel. This is not the case in quasifission which is known to preserve a strong memory of the entrance channel properties. As a result, understanding the interplay between the entrance and exit channels requires a large amount of experimental systematic studies. These include investigations of the role of beam energy [12, 18], fissility of the compound nucleus [19, 20], deformation of the target [12, 21–24], spherical shells of the collision partners [25, 26], and the neutron-to-proton ratio N/Z of the compound nucleus [27, 28].

On the theory side, quasifission has been studied with various approaches. This includes classical methods such as a transport model [29], the dinuclear system model [30–33], and models based on the Langevin equation [34–38]. Microscopic approaches such as quantum molecular dynamics [39–41] and the time-dependent Hartree-Fock (TDHF) theory [14, 15, 27, 38, 42–51] have also been used. See [52–55] for recent reviews on TDHF.

An advantage of microscopic calculations is that their only inputs are the parameters of the energy density functional describing the interaction between the nucleons. Since the latter are usually fitted on nuclear structure properties only, such calculations do not require any parameter determined from reaction mechanisms, such as nucleus-nucleus potentials. In addition, TDHF calculations treat both reaction mechanisms and structure properties on the same footing. This is important for reactions with actinide targets which exhibit a strong quadrupole deformation.

Indeed, the outcome of the calculations strongly depend on the orientation of the nuclei. For instance, TDHF calculations of ^{40}Ca+^{238}U reaction showed that only collisions with the side of the ^{238}U could lead to configurations which are compact enough to enable fusion [14]. This is at variance with collisions with the tip of ^{238}U which seem to always lead to a fast quasi-fission (after $\sim 5-10$ zeptoseconds of contact time) as long as contact between collision partners is achieved. A remarkable observation of this work was the systematic production of lead nuclei ($Z=82$), known to possess a strong spherical proton shell gap, in tip collisions only, showing a strong influence of orientation dependent shell effects in the production of the fragments. Such influence of shell effects was proposed to explain peaks in fragment mass distributions [11, 12, 14], but experimental confirmation came only recently with the observation of a peak of quasifission fragments at $Z=82$ protons from $X-$ray measurements [15].

Deformed shell effects in the region of ^{100}Zr have also been invoked to interpret the outcome of TDHF simulations of ^{40,48}Ca+^{238}U,^{249}Bk collisions [44, 46]. It is then natural to wonder if other shell effects, spherical or deformed, could be driving the dinuclear system out of its compact shape, into quasifission. Potential candidates are shell effects known to influence the outcome of fission reaction. It has recently been proposed that octupole deformed shell effects, in particular with Z or $N=52-56$, are the main driver to asymmetric fission [56, 57]. The fact that ^{208}Pb can easily acquire an oc-

* umar@compsci.cas.vanderbilt.edu
† cedric.simenel@anu.edu.au

tupole deformation (its first excited state is an 3^- octupole vibration) is compatible with this interpretation. Note also that some superheavy nuclei like ^{294}Og are expected to encounter super asymmetric fission and produce a heavy fragment around ^{208}Pb [58–61], conforting the idea that quasifission valleys could match fission ones.

In this work we study the ^{48}Ca+^{249}Nk reaction at $E_{cm} = 234$ MeV with the TDHF approach. Previsous TDHF studies of quasifission with actinide targets were restricted to one or two orientations of the target to limit computational time. However, to allow possible comparison with experimental data, it is important to simulate a range of orientations in addition to the usual tip and side configurations. We therefore performed systematic simulations, spanning both a range of orientations and a range of angular momenta. This allow us to study correlations between, e.g., mass, angle, kinetic energy, as well as to predict distributions of neutron and proton numbers at the mean-field level. This distributions are used to identify potential shell gaps driving quasifission. The method is described in section II. The results are discussed in section III. We then conclude in section IV.

II. METHOD

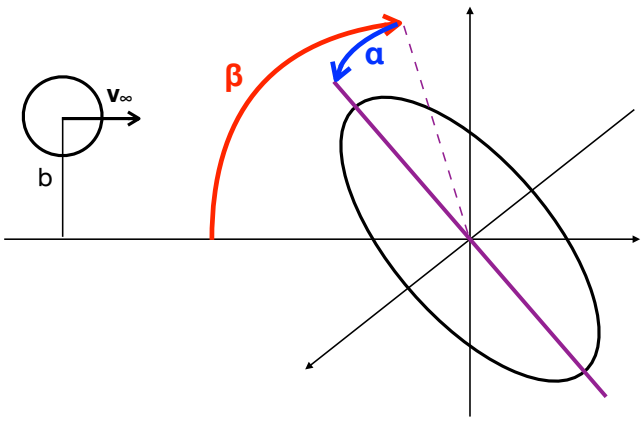

FIG. 1. (Color online) Schematic representation of the initial configuration for an impact parameter b and a velocity vector $\mathbf{v}_\infty$ defining the collision plane and the collision axis. The orientation of the target is defined by the angles β (rotation around the axis perpendicular to the reaction plane) and α (rotation around the collision axis).

Assuming the ^{249}Bk nucleus to be axially symmetric with no octupole deformation, the cross-section or yield for a specific reaction channel ξ is proportional to

$$\sigma_\xi \propto \sum_L (2L+1) \int_0^{\frac{\pi}{2}} d\beta \, \sin\beta \int_0^{\pi} d\alpha \, P_L^{(\xi)}(\beta,\alpha). \quad (1)$$

$P_L^{(\xi)}(\beta,\alpha)$ is the probability for the reaction channel ξ and an orientation of the target defined by the rotation angles β and α (see Fig. 1). The orientation of the deformation axis is obtained by applying first a rotation of an angle β around the axis perpendicular to the reaction plane, and then a rotation of an angle α around the collision axis.

The TDHF calculations are performed for a range of orbital angular momenta $L_i\hbar$ with $\{L_i\} = \{0, 10, 20 \cdots N_L\}$ and $N_L = 12$ or 13, depending on the orientation (some orientations lead to quasi-elastic collisions at $L = 120$, in which case $L = 130$ is not computed). The first term is then replaced by

$$\sum_L (2L+1) \rightarrow \sum_{i=1}^{N_L} K_i \quad \text{with} \quad K_i = \sum_{L=L_i-\Delta_i^-}^{L_i+\Delta^+} (2L+1),$$

where $\Delta^+ = 5$, $\Delta_1^- = 0$ and $\Delta_{i\neq}1 = 4$.

The double integral in Eq. 1 is computationally too demanding. The integral over α is then replaced by a sum over probabilities for $\alpha = 0$ and π. Equivalently, we can ignore α and extend the integral over β up to π. We then define the probability

$$\tilde{P}_{L_i}^{(\xi)}(\beta) = \begin{cases} P_{L_i}^{(\xi)}(\beta,0) \text{ if } \beta \leq \frac{\pi}{2} \\ P_{L_i}^{(\xi)}(\pi-\beta,\pi) \text{ if } \beta > \frac{\pi}{2} \end{cases} .$$

The remaining integral over β is discretised with $N_\beta = 12$ angles $\{\beta_n\} = \{0, 15, 30, \cdots 165\}$ deg. We can finally write the approximate cross-section as

$$\sigma_\xi \simeq \sum_{i=1}^{N_L} K_i \sum_{n=1}^{N_\beta} C_n \tilde{P}_{L_i}^{(\xi)}(\beta_n) \quad (2)$$

where we have defined

$$C_n = \begin{cases} 2(1-\cos\delta) \text{ if } n = 1 \\ \cos(\beta_n - \delta) - \cos(\beta_n + \delta) \text{ if } n > 1 \end{cases}$$

with $\delta = 7.5$ deg. Note that, because of its semi-classical behaviour, the TDHF theory leads to probabilities $\tilde{P}_{L_i}^{(\xi)}(\beta_n) = 0$ or 1 for the reaction channel ξ and for a given orientation and angular momentum.

III. RESULTS

A. Quasifission characteristics

The ^{48}Ca+^{249}Bk at $E_{cm} = 234$ MeV has been studied as a function of the orientation β of the target (see Fig. 1) and as a function of orbital angular momentum L, given in units of $\hbar$. Figure 2 shows a typical example of density evolution for

Side collisions ($\beta \sim 90$ degrees) lead to fusion.

Energy/deformation fast/slow quasifission [64] Fast quasifission [20]

IV. CONCLUSIONS

ACKNOWLEDGMENTS

This work has been supported by the U.S. Department of Energy under grant No. DE-SC0013847 with Vanderbilt Uni-

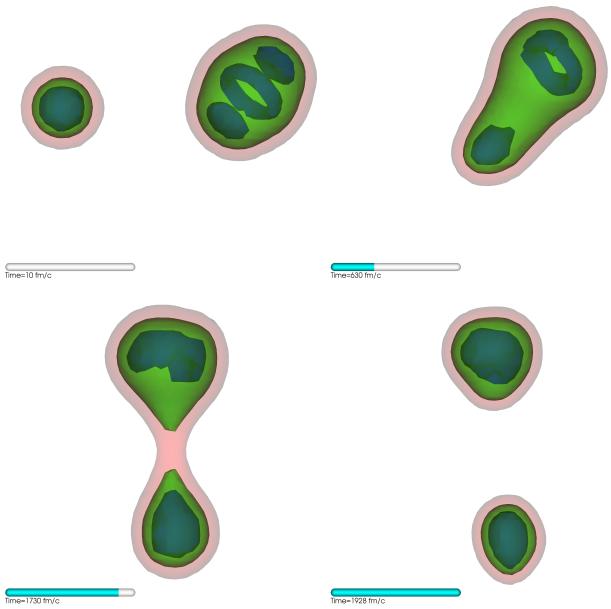

FIG. 2. (Color online) Isodensity surfaces at $\rho = XX$, YY and ZZ fm^{-3} in blue, green and pink, respectively, shown at time $t = 10$ (a), 630 (b), 1730 (c) and 1928 fm/c (d) for an initial orientation $\beta = WWW$ degrees and an angular momentum $L\hbar = NN\hbar$. For visualisation purpose, the reaction plane is QQ degrees off the plane of the page.

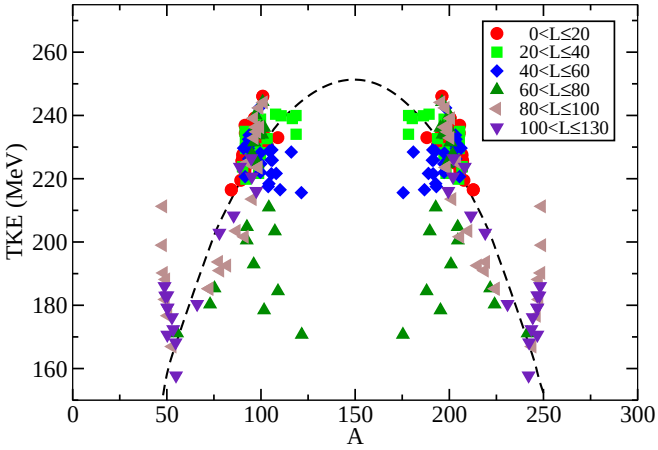

FIG. 3. (Color online) Total kinetic energy of the fragments as a function of their mass ratio. The curve corresponds to the Viola systematics [62, 63].

versity and by the Australian Research Council Discovery Project (project numbers DP160101254 and DP190100256) funding schemes.

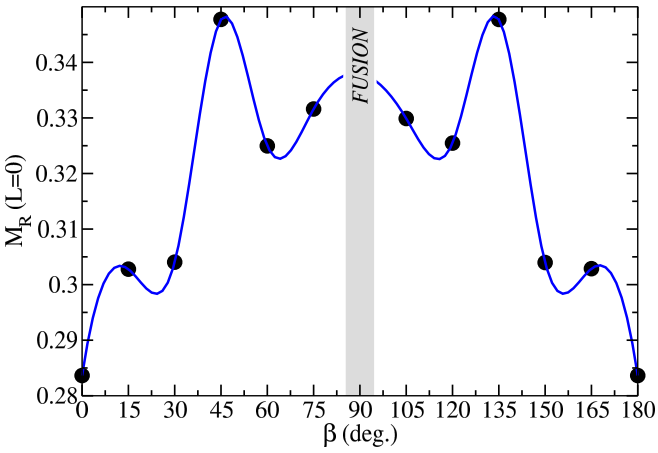

FIG. 4. (Color online).Mass ratio M_R as a function of orientation angle β for central collisions. Fusion is indicated by the shaded area.

[1] B. Heusch, C. Volant, H. Freiesleben, R. P. Chestnut, K. D. Hildenbrand, F. Pühlhofer, W. F. W. Schneider, B. Kohlmeyer, and W. Pfeffer, "The reaction mechanism in the system ^{132}Xe+^{56}Fe at 5.73 MeV/u: Evidence for a new type of strongly damped collisions," Z. Phys. A **288**, 391–400 (1978).

[2] B. B. Back, H.-G. Clerc, R. R. Betts, B. G. Glagola, and B. D. Wilkins, "Observation of Anisotropy in the Fission Decay of Nuclei with Vanishing Fission Barrier," Phys. Rev. Lett. **46**, 1068–1071 (1981).

[3] R. Bock, Y. T. Chu, M. Dakowski, A. Gobbi, E. Grosse, A. Olmi, H. Sann, D. Schwalm, U. Lynen, W. Müller, S. Bjørnholm, H. Esbensen, W. Wölfli, and E. Morenzoni, "Dynamics of the fusion process," Nucl. Phys. A **388**, 334–380 (1982).

[4] C.-C. Sahm, H.-G. Clerc, K.-H. Schmidt, W. Reisdorf, P. Armbruster, F. P. Heßberger, J. G. Keller, G. Münzenberg, and D. Vermeulen, "Hindrance of fusion in central collisions of heavy symmetric nuclear systems," Z. Phys. A **319**, 113–118 (1984).

[5] H. Gäggeler, T. Sikkeland, G. Wirth, W. Brüchle, W. Bögl, G. Franz, G. Herrmann, J. V. Kratz, M. Schädel, K. Sümmerer, and W. Weber, "Probing sub-barrier fusion and extra-push by measuring fermium evaporation residues in different heavy ion reactions," Z. Phys. A **316**, 291–307 (1984).

[6] K.-H. Schmidt and W. Morawek, "The conditions for the synthesis of heavy nuclei," Rep. Prog. Phys. **54**, 949 (1991).

[7] J. Khuyagbaatar, H. M. David, D. J. Hinde, I. P. Carter, K. J. Cook, M. Dasgupta, Ch. E. Düllmann, D. Y. Jeung, B. Kindler, B. Lommel, D. H. Luong, E. Prasad, D. C. Rafferty, C. Sengupta, C. Simenel, E. C. Simpson, J. F. Smith, K. Vo-Phuoc, J. Walshe, A. Wakhle, E. Williams, and A. Yakushev, "Nuclear structure dependence of fusion hindrance in heavy element synthesis," Phys. Rev. C **97**, 064618 (2018).

[8] J. Tõke, R. Bock, G. X. Dai, A. Gobbi, S. Gralla, K. D. Hildenbrand, J. Kuzminski, W. F. J. Müller, A. Olmi, H. Stelzer, B. B. Back, and S. Bjørnholm, "Quasi-fission: The mass-drift mode in heavy-ion reactions," Nucl. Phys. A **440**, 327–365 (1985).

[9] W. Q. Shen, J. Albinski, A. Gobbi, S. Gralla, K. D. Hilden-

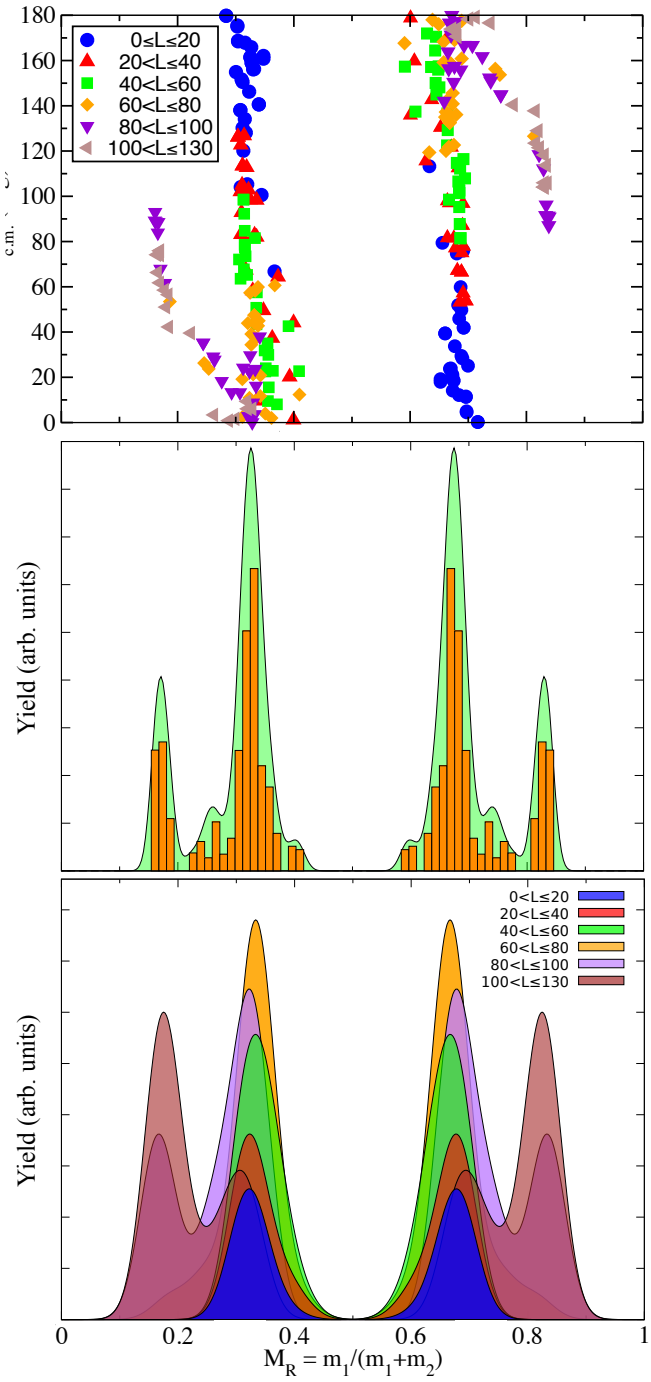

FIG. 5. (Color online). (a) Distribution of scattering angle $\theta_c m$ versus mass ratio M_R (MAD). The colors correspond to different ranges of angular momenta. (b) Fragment mass yield (histogram). The solid line gives a smooth representation of the histogram using gnuplot k-density function with width XX. (c) Mass yields obtained for different ranges of angular momenta.

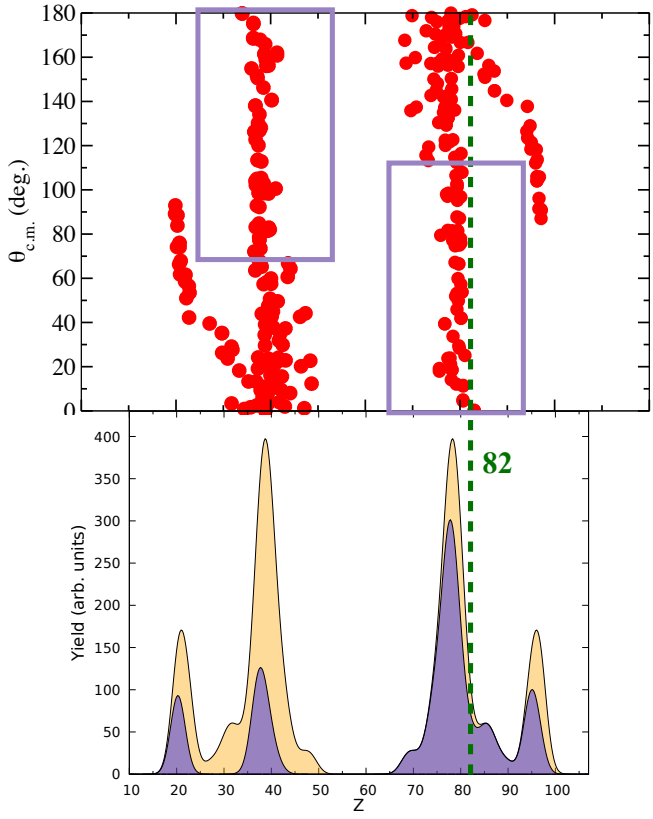

FIG. 6. (Color online). (a) Distribution of scattering angle θ_{cm} versus proton number Z (ZAD). (b) Fragment proton number yield without (black solid line) and with angular cut $\theta_{cm} > 70$ degrees (dashed line). The vertical lines represent potential proton shell gaps.

.

brand, N. Herrmann, J. Kuzminski, W. F. J. Müller, H. Stelzer, J. Tõke, B. B. Back, S. Bjørnholm, and S. P. Sørensen, "Fission and quasifission in U-induced reactions," Phys. Rev. C **36**, 115–142 (1987).

[10] R. du Rietz, D. J. Hinde, M. Dasgupta, R. G. Thomas, L. R. Gasques, M. Evers, N. Lobanov, and A. Wakhle, "Predominant Time Scales in Fission Processes in Reactions of S, Ti and Ni with W: Zeptosecond versus Attosecond," Phys. Rev. Lett. **106**, 052701 (2011).

[11] M. G. Itkis, J. Äystö, S. Beghini, A. A. Bogachev, L. Corradi, O. Dorvaux, A. Gadea, G. Giardina, F. Hanappe, I. M. Itkis, M. Jandel, J. Kliman, S. V. Khlebnikov, G. N. Kniajeva, N. A. Kondratiev, E. M. Kozulin, L. Krupa, A. Latina, T. Materna, G. Montagnoli, Yu. Ts. Oganessian, I. V. Pokrovsky, E. V. Prokhorova, N. Rowley, V. A. Rubchenya, A. Ya. Rusanov, R. N. Sagaidak, F. Scarlassara, A. M. Stefanini, L. Stuttge, S. Szilner, M. Trotta, W. H. Trzaska, D. N. Vakhtin, A. M. Vinodkumar, V. M. Voskressenski, and V. I. Zagrebaev, "Shell effects in fission and quasi-fission of heavy and superheavy nuclei," Nucl. Phys. A **734**, 136–147 (2004).

[12] K. Nishio, H. Ikezoe, S. Mitsuoka, I. Nishinaka, Y. Nagame, Y. Watanabe, T. Ohtsuki, K. Hirose, and S. Hofmann, "Effects of nuclear orientation on the mass distribution of fission fragments in the reaction of ^{36}S + ^{238}U," Phys. Rev. C **77**, 064607 (2008).

[13] E. M. Kozulin, G. N. Knyazheva, S. N. Dmitriev, I. M. Itkis, M. G. Itkis, T. A. Loktev, K. V. Novikov, A. N. Baranov, W. H. Trzaska, E. Vardaci, S. Heinz, O. Beliuskina, and S. V. Khlebnikov, "Shell effects in damped collisions of ^{88}Sr with ^{176}Yb at the Coulomb barrier energy," Phys. Rev. C **89**, 014614 (2014).

[14] A. Wakhle, C. Simenel, D. J. Hinde, M. Dasgupta, M. Evers,

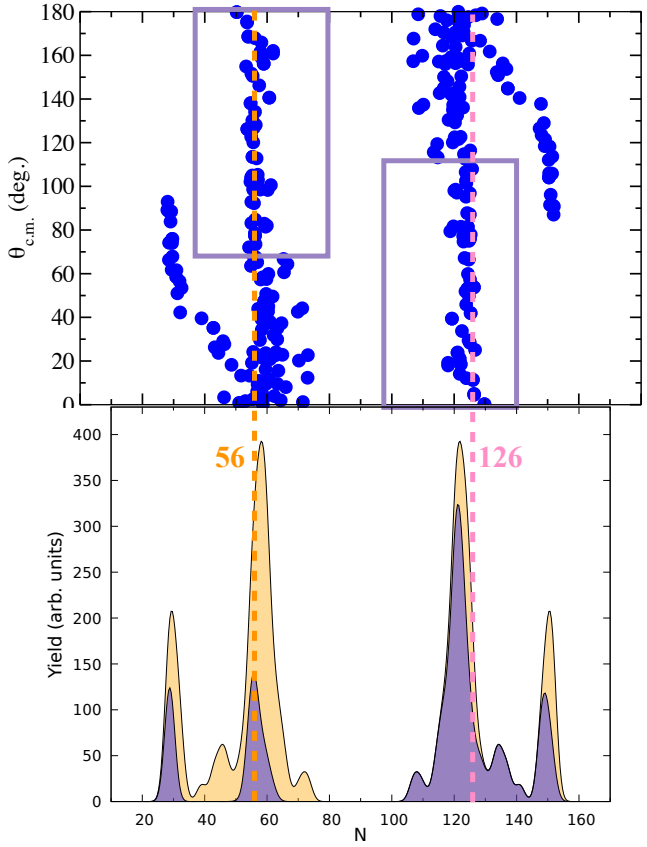

FIG. 7. (Color online). (a) Distribution of scattering angle θ_{cm} versus neutron number N (NAD). (b) Fragment neutron number yield without (black solid line) and with angular cut $\theta_{cm} > 70$ degrees (dashed line). The vertical lines represent potential neutron shell gaps.

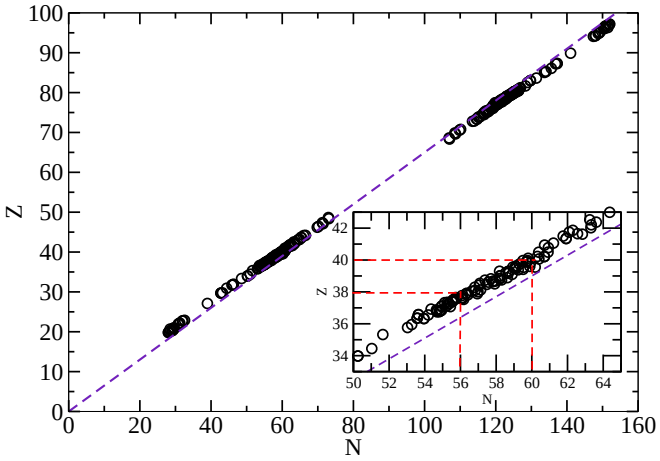

FIG. 8. (Color online). Distribution of proton number Z versus neutron number N of the fragments. The dashed line represents the N/Z ratio of the compound nucleus. The inset is a zoom around the light fragment. Thin dashed lines indicate the positions of ^{94}Sr ($Z = 38$, $N = 56$) and ^{100}Zr ($Z = 40$, $N = 60$).

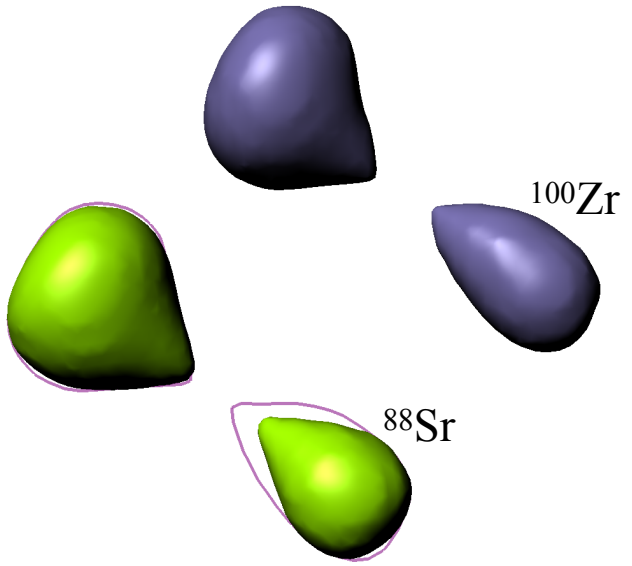

FIG. 9. (Color online). Isodensity surfaces at $\rho = 0.1$ fm^{-3} for $L = NN$ and $\beta = XXX$ degrees (top), and $L = MM$ and $\beta = YYY$ degrees (bottom), just after breaking of the neck. The light fragment (right) in the top is a ^{94}Sr ($Z = 38$, $N = 56$) and a ^{100}Zr ($Z = 40$, $N = 60$) in the bottom. The contour line in the bottom represents the same density as in the top.

D. H. Luong, R. du Rietz, and E. Williams, "Interplay between Quantum Shells and Orientation in Quasifission," Phys. Rev. Lett. **113**, 182502 (2014).

[15] M. Morjean, D. J. Hinde, C. Simenel, D. Y. Jeung, M. Airiau, K. J. Cook, M. Dasgupta, A. Drouart, D. Jacquet, S. Kalkal, C. S. Palshetkar, E. Prasad, D. Rafferty, E. C. Simpson, L. Tassan-Got, K. Vo-Phuoc, and E. Williams, "Evidence for the Role of Proton Shell Closure in Quasifission Reactions from X–Ray Fluorescence of Mass–Identified Fragments," Phys. Rev. Lett. **119**, 222502 (2017).

[16] M. Veselsky, J. Klimo, Yu-Gang Ma, and G. A. Souliotis, "Constraining the equation of state of nuclear matter from fusion hindrance in reactions leading to the production of superheavy elements," Phys. Rev. C **94**, 064608 (2016).

[17] H. Zheng, S. Burrello, M. Colonna, D. Lacroix, and G. Scamps, "Connecting the nuclear equation of state to the interplay between fusion and quasifission processes in low-energy nuclear reactions," Phys. Rev. C **98**, 024622 (2018).

[18] K. Nishio, S. Mitsuoka, I. Nishinaka, H. Makii, Y. Wakabayashi, H. Ikezoe, K. Hirose, T. Ohtsuki, Y. Aritomo, and S. Hofmann, "Fusion probabilities in the reactions ^{40,48}Ca + ^{238}U at energies around the Coulomb barrier," Phys. Rev. C **86**, 034608 (2012).

[19] C. J. Lin, R. du Rietz, D. J. Hinde, M. Dasgupta, R. G. Thomas, M. L. Brown, M. Evers, L. R. Gasques, and M. D. Rodriguez, "Systematic behavior of mass distributions in ^{48}Ti-induced fission at near-barrier energies," Phys. Rev. C **85**, 014611 (2012).

[20] R. du Rietz, E. Williams, D. J. Hinde, M. Dasgupta, M. Evers, C. J. Lin, D. H. Luong, C. Simenel, and A. Wakhle, "Mapping quasifission characteristics and timescales in heavy element formation reactions," Phys. Rev. C **88**, 054618 (2013).

[21] D. J. Hinde, M. Dasgupta, J. R. Leigh, J. P. Lestone, J. C. Mein, C. R. Morton, J. O. Newton, and H. Timmers, "Fusion-Fission versus Quasifission: Effect of Nuclear Orientation," Phys. Rev. Lett. **74**, 1295–1298 (1995).

[22] D. J. Hinde, M. Dasgupta, J. R. Leigh, J. C. Mein, C. R. Morton,

J. O. Newton, and H. Timmers, "Conclusive evidence for the influence of nuclear orientation on quasifission," Phys. Rev. C **53**, 1290–1300 (1996).

[23] G. N. Knyazheva, E. M. Kozulin, R. N. Sagaidak, A. Yu. Chizhov, M. G. Itkis, N. A. Kondratiev, V. M. Voskressensky, A. M. Stefanini, B. R. Behera, L. Corradi, E. Fioretto, A. Gadea, A. Latina, S. Szilner, M. Trotta, S. Beghini, G. Montagnoli, F. Scarlassara, F. Haas, N. Rowley, P. R. S. Gomes, and A. Szanto de Toledo, "Quasifission processes in ^{40,48}Ca + ^{144,154}Sm reactions," Phys. Rev. C **75**, 064602 (2007).

[24] D. J. Hinde, R. G. Thomas, R. du Rietz, A. Diaz-Torres, M. Dasgupta, M. L. Brown, M. Evers, L. R. Gasques, R. Rafiei, and M. D. Rodriguez, "Disentangling Effects of Nuclear Structure in Heavy Element Formation," Phys. Rev. Lett. **100**, 202701 (2008).

[25] C. Simenel, D. J. Hinde, R. du Rietz, M. Dasgupta, M. Evers, C. J. Lin, D. H. Luong, and A. Wakhle, "Influence of entrance-channel magicity and isospin on quasi-fission," Phys. Lett. B **710**, 607–611 (2012).

[26] G. Mohanto, D. J. Hinde, K. Banerjee, M. Dasgupta, D. Y. Jeung, C. Simenel, E. C. Simpson, A. Wakhle, E. Williams, I. P. Carter, K. J. Cook, D. H. Luong, C. S. Palshetkar, and D. C. Rafferty, "Interplay of spherical closed shells and N/Z asymmetry in quasifission dynamics," Phys. Rev. C **97**, 054603 (2018).

[27] K. Hammerton, Z. Kohley, D. J. Hinde, M. Dasgupta, A. Wakhle, E. Williams, V. E. Oberacker, A. S. Umar, I. P. Carter, K. J. Cook, J. Greene, D. Y. Jeung, D. H. Luong, S. D. McNeil, C. S. Palshetkar, D. C. Rafferty, C. Simenel, and K. Stiefel, "Reduced quasifission competition in fusion reactions forming neutron-rich heavy elements," Phys. Rev. C **91**, 041602(R) (2015).

[28] K. Hammerton, D. J. Morrissey, Z. Kohley, D. J. Hinde, M. Dasgupta, A. Wakhle, E. Williams, I. P. Carter, K. J. Cook, J. Greene, D. Y. Jeung, D. H. Luong, S. D. McNeil, C. Palshetkar, D. C. Rafferty, C. Simenel, and K. Stiefel, "Entrance channel effects on the quasifission reaction channel in Cr+W systems," Phys. Rev. C **99**, 054621 (2019).

[29] A. Diaz-Torres, G. G. Adamian, N. V. Antonenko, and W. Scheid, "Quasifission process in a transport model for a dinuclear system," Phys. Rev. C **64**, 024604 (2001).

[30] G. G. Adamian, N. V. Antonenko, and W. Scheid, "Characteristics of quasifission products within the dinuclear system model," Phys. Rev. C **68**, 034601 (2003).

[31] Minghui Huang, Zaiguo Gan, Xiaohong Zhou, Junqing Li, and W. Scheid, "Competing fusion and quasifission reaction mechanisms in the production of superheavy nuclei," Phys. Rev. C **82**, 044614 (2010).

[32] X. J. Bao, Y. Gao, J. Q. Li, and H. F. Zhang, "Theoretical study of the synthesis of superheavy nuclei using radioactive beams," Phys. Rev. C **91**, 064612 (2015).

[33] S. Q. Guo, Y. Gao, J. Q. Li, and H. F. Zhang, "Dynamical deformation in heavy ion reactions and the characteristics of quasifission products," Phys. Rev. C **96**, 044622 (2017).

[34] Valery Zagrebaev and Walter Greiner, "Unified consideration of deep inelastic, quasi-fission and fusion-fission phenomena," J. Phys. G **31**, 825 (2005).

[35] Y. Aritomo, "Analysis of dynamical processes using the mass distribution of fission fragments in heavy-ion reactions," Phys. Rev. C **80**, 064604 (2009).

[36] Y. Aritomo, K. Hagino, K. Nishio, and S. Chiba, "Dynamical approach to heavy-ion induced fission using actinide target nuclei at energies around the Coulomb barrier," Phys. Rev. C **85**, 044614 (2012).

[37] A. V. Karpov and V. V. Saiko, "Modeling near-barrier collisions of heavy ions based on a Langevin-type approach," Phys. Rev. C **96**, 024618 (2017).

[38] K. Sekizawa and K. Hagino, "Time-dependent Hartree-Fock plus Langevin approach for hot fusion reactions to synthesize the $Z = 120$ superheavy element," Phys. Rev. C **99**, 051602 (2019).

[39] Kai Wen, Fumihiko Sakata, Zhu-Xia Li, Xi-Zhen Wu, Ying-Xun Zhang, and Shan-Gui Zhou, "Non-Gaussian Fluctuations and Non-Markovian Effects in the Nuclear Fusion Process: Langevin Dynamics Emerging from Quantum Molecular Dynamics Simulations," Phys. Rev. Lett. **111**, 012501 (2013).

[40] Ning Wang and Lu Guo, "New neutron-rich isotope production in ^{154}Sm+^{160}Gd," Phys. Lett. B **760**, 236–241 (2016).

[41] Kai Zhao, Zhuxia Li, Yingxun Zhang, Ning Wang, Qingfeng Li, Caiwan Shen, Yongjia Wang, and Xizhen Wu, "Production of unknown neutron–rich isotopes in ^{238}U+^{238}U collisions at near–barrier energy," Phys. Rev. C **94**, 024601 (2016).

[42] Cédric Golabek and Cédric Simenel, "Collision Dynamics of Two ^{238}U Atomic Nuclei," Phys. Rev. Lett. **103**, 042701 (2009).

[43] David J. Kedziora and Cédric Simenel, "New inverse quasifission mechanism to produce neutron-rich transfermium nuclei," Phys. Rev. C **81**, 044613 (2010).

[44] V. E. Oberacker, A. S. Umar, and C. Simenel, "Dissipative dynamics in quasifission," Phys. Rev. C **90**, 054605 (2014).

[45] A. S. Umar, V. E. Oberacker, and C. Simenel, "Shape evolution and collective dynamics of quasifission in the time-dependent Hartree-Fock approach," Phys. Rev. C **92**, 024621 (2015).

[46] A. S. Umar, V. E. Oberacker, and C. Simenel, "Fusion and quasifission dynamics in the reactions ^{48}Ca + ^{249}Bk and ^{50}Ti + ^{249}Bk using a time-dependent Hartree-Fock approach," Phys. Rev. C **94**, 024605 (2016).

[47] Kazuyuki Sekizawa and Kazuhiro Yabana, "Time-dependent Hartree-Fock calculations for multinucleon transfer and quasifission processes in the ^{64}Ni + ^{238}U reaction," Phys. Rev. C **93**, 054616 (2016).

[48] Chong Yu and Lu Guo, "Angular momentum dependence of quasifission dynamics in the reaction ^{48}Ca+^{244}Pu," Sci. China Phys. **60**, 092011 (2017).

[49] S. Ayik, B. Yilmaz, O. Yilmaz, A. S. Umar, and G. Turan, "Multinucleon transfer in central collisions of ^{238}U + ^{238}U," Phys. Rev. C **96**, 024611 (2017).

[50] Kazuyuki Sekizawa, "Enhanced nucleon transfer in tip collisions of ^{238}U + ^{124}Sn," Phys. Rev. C **96**, 041601(R) (2017).

[51] A. Wakhle, K. Hammerton, Z. Kohley, D. J. Morrissey, K. Stiefel, J. Yurkon, J. Walshe, K. J. Cook, M. Dasgupta, D. J. Hinde, D. J. Jeung, E. Prasad, D. C. Rafferty, C. Simenel, E. C. Simpson, K. Vo-Phuoc, J. King, W. Loveland, and R. Yanez, "Capture cross sections for the synthesis of new heavy nuclei using radioactive beams," Phys. Rev. C **97**, 021602 (2018).

[52] Cédric Simenel, "Nuclear quantum many-body dynamics," Eur. Phys. J. A **48**, 152 (2012).

[53] C. Simenel and A. S. Umar, "Heavy–ion collisions and fission dynamics with the time–dependent Hartree-Fock theory and its extensions," Prog. Part. Nucl. Phys. **103**, 19–66 (2018).

[54] Kazuyuki Sekizawa, "TDHF Theory and Its Extensions for the Multinucleon Transfer Reaction: A Mini Review," Front. Phys. **7**, 20 (2019).

[55] P. D. Stevenson and M. C. Barton, "Low–energy heavy-ion reactions and the Skyrme effective interaction," Prog. Part. Nucl. Phys. **104**, 142–164 (2019).

[56] Guillaume Scamps and Cédric Simenel, "Impact of pear-shaped fission fragments on mass-asymmetric fission in actinides," Na-

ture **564**, 382–385 (2018).

[57] G. Scamps and C. Simenel, "Effect of shell structure on the fission of sub-lead nuclei," Arxiv:1904.012705 (2019).

[58] D. N. Poenaru and R. A. Gherghescu, "α decay and cluster radioactivity of nuclei of interest to the synthesis of $Z = 119, 120$ isotopes," Phys. Rev. C **97**, 044621 (2018).

[59] M. Warda, A. Zdeb, and L. M. Robledo, "Cluster radioactivity in superheavy nuclei," Phys. Rev. C **98**, 041602 (2018).

[60] Zachary Matheson, Samuel A. Giuliani, Witold Nazarewicz, Jhilam Sadhukhan, and Nicolas Schunck, "Cluster radioactivity of $^{294}_{118}\mathrm{Og}_{176}$," Phys. Rev. C **99**, 041304 (2019).

[61] Y. L. Zhang and Y. Z. Wang, "Systematic study of cluster radioactivity of superheavy nuclei," Phys. Rev. C **97**, 014318 (2018).

[62] V. E. Viola, K. Kwiatkowski, and M. Walker, "Systematics of fission fragment total kinetic-energy release," Phys. Rev. C **31**, 1550–1552 (1985).

[63] D. J. Hinde, J. R. Leigh, J. J. M. Bokhorst, J. O. Newton, R. L. Walsh, and J. W. Boldeman, "Mass-split dependence of the pre- and post-scission neutron multiplicities for fission of ^{251}Es," Nucl. Phys. A **472**, 318–332 (1987).

[64] D. J. Hinde, D. Y. Jeung, E. Prasad, A. Wakhle, M. Dasgupta, M. Evers, D. H. Luong, R. du Rietz, C. Simenel, E. C. Simpson, and E. Williams, "Sub—barrier quasifission in heavy element formation reactions with deformed actinide target nuclei," Phys. Rev. C **97**, 024616 (2018).